PHYSICAL REVIEW B VOLUME 47, NUMBER 16 15 APRIL 1993-II

Growth and structure of Fe and Co thin films on Cu(111), Cu(100), and Cu(110): A comprehensive study of metastable film growth

M. T. Kief and W. F. Egelhoff, Jr.
Surface and Microanalysis Science Division, National Institute of Standards and Technology, Gaithersburg, Maryland 20899
(Received 2 November 1992)

The growth and structure of Fe and Co thin films on single-crystal Cu(111), Cu(100), and Cu(110) substrates have been investigated using x-ray-photoelectron and Auger electron forward scattering, CO-titration, low-energy electron diffraction, and reflection high-energy electron diffraction. The motivation for this study is to understand the role of surface structure and kinetics in the growth of metal films on metal substrates. The effect of varying substrate growth temperatures between 80 and 450 K plays a prominent role in determining both the film morphology and crystalline phase. Nonideal film growth, including agglomeration of Co and Fe and surface segregation of Cu, is the rule rather than the exception. Simple considerations of surface diffusion and surface free-energy differences provide a basis for understanding why layer-by-layer growth is unlikely to occur in these systems and should not be expected in many other metastable film-substrate systems.

I. INTRODUCTION

Substantial research has sought to understand the diverse structural and magnetic properties of thin films of Fe and Co grown on Cu. These systems are employed in the research fields of surface magnetism, low-dimensional magnetism, magneto-optics, giant magnetoresistance, and many others (see Ref. 1 and references therein). The applications of this research span from magnetic recording media and recording heads to nonvolatile memory chips. Unfortunately, the results of these research studies have often been contradictory. This confusion is largely due to an inadequate understanding of the film growth, film morphology, and the delicate interplay between thin-film structure and magnetic properties. Therefore, it is timely to examine the building blocks of these structures namely, monolayer films of Fe and Co epitaxially grown on Cu(111), Cu(100), and Cu(110).

We report the structure and morphology of Fe and Co films prepared by molecular-beam epitaxy on single-crystal Cu substrates. We interpret these results in terms of the film-growth dynamics. To examine the effects of substrate structure, the film-growth mode has been studied on Cu(100), Cu(100), and Cu(111) with varying substrate preparations. To explore the effects of varying growth kinetics upon the system structure, films were grown at substrate temperatures ranging from 80 to 450 K. Presented here is a systematic and comprehensive structural study of these metastable systems using several complementary techniques including x-ray-photoelectron and Auger electron forward scattering, low-energy electron diffraction (LEED), reflection high-energy electron diffraction (RHEED) and CO titration.

Epitaxial growth of a metal film on a metal substrate is often categorized according to three standard models: two-dimensional or Frank–van der Merwe (FM) growth, three-dimensional or Volmer-Weber (VW) growth, and two-dimensional followed by three-dimensional or Stranski-Krastanov (SK) growth. According to the quasiequilibrium description by Bauer,[2] these three growth modes are governed by the surface free energies, the interface free energy, and the strain energy. The deposited film will grow in two dimensions or layer-by-layer (FM) if

$$\sigma_f - \sigma_s + \sigma_i + \sigma_e < 0 \ , \tag{1}$$

where σ_f is the deposited film surface free energy, σ_s is the substrate surface free energy, σ_i is the interface surface free energy, and σ_e is the strain energy. Otherwise, the film nucleates as three-dimensional clusters (VW). In the event that the inequality reverses with film thickness, layer-by-layer growth is followed by three-dimensional growth (SK).

A common goal in epitaxy is to produce two-dimensional film structures with a particular crystallographic phase and orientation. To attain this goal, we often desire FM growth. However, FM growth is difficult to obtain for Fe/Cu and Co/Cu because the surface free energies[3] of Co (2.709 $\mathrm{J\,m^{-2}}$) and Fe (2.939 $\mathrm{J\,m^{-2}}$) are significantly larger than the surface free energy of Cu (1.934 $\mathrm{J\,m^{-2}}$). In addition, since the heats of mixing for both Fe-Cu and Co-Cu are endothermic,[4] we can expect the interface free energies costs to be unfavorable. According to Eq. (1), the initial equilibrium growth of Fe and Co on Cu should be similar to VW, not FM as has been frequently reported.[5–24]

Furthermore, the quasiequilibrium VW growth mode predicted by Eq. (1) is frequently not obtained. Nonequilibrium growth can occur because kinetic factors (such as surface diffusion) are too slow. The actual film growth can result in departures from equilibrium structures and crystallographic changes [e.g., Fe/Cu(111)]. In addition, the three idealized growth modes neglect the possibility that substrate atoms can be mobile and may segregate to the surface during film growth. The importance of surface segregation is exemplified by its

Work of the U. S. Government
Not subject to U. S. copyright

DOCKET ALARM Find authenticated court documents without watermarks at docketalarm.com.

widespread prediction and observation in metallic alloys.[4,25–27]

To understand whether equilibrium growth can be expected, we must identify the controlling processes. Three important processes relevant to metal-film on metal-substrate growth are (i) surface adatom diffusion, (ii) substrate surface segregation, and (iii) film/substrate interdiffusion. These processes are activated by increasing the substrate temperature during film growth. For a process to be significant, its rate should be compared to the film deposition rate, which is typically around 1 monolayer/min. In addition, it is essential to recognize that surface diffusion varies with crystal face and surface quality as well as element.

Activation energy barriers for surface diffusion have been measured for some metal/metal systems.[28–48] Typically, the measured surface diffusion barrier ranges from near 0.1 to 0.9 eV for different metals and different crystal faces. The surface diffusion process is assumed to follow an Arrhenius diffusion law, $D_0\exp(-E_d/k_BT)$, where E_d is the activation energy, k_B is the Boltzmann constant, T is the temperature, and with a typical preexponential D_0 of $\sim 10^{-3}$ cm^2/s.[28,29,32] Activation energies of 0.1–0.9 eV translate to about 40–350 K for an adatom mobility of 1 hop/s. As an example of the crystal face dependence, Ir self-diffusion has been determined to have activation energies of 0.27 eV for Ir/Ir(111),[30] 0.7 eV for Ir/Ir(110),[48] and 0.84 eV for Ir/Ir(100).[31]

The experimentally determined activation energy for self-diffusion on Cu(100), has been reported to be 0.28±0.06 (Ref. 49), 0.39±0.06 (Ref. 50), and ~0.48 eV.[51] Since other experimental surface diffusion data for Cu data are not available, we must rely solely upon theoretical estimates for self-diffusion on Cu(111) and Cu(110). Recent effective-medium calculations predict diffusion barriers for Cu(111), Cu(110), and Cu(100) of 0.13, 0.18, and 0.21 eV, respectively.[52,53] Since surface diffusion barrier energies are not available for many materials, it is useful to have a simple means to approximate them. An estimate of the diffusion barrier can be obtained by scaling the activation energy of an unknown material to a known material using the cohesive energies. Using the cohesive energy ratio for Cu/Ir=0.502 (Ref. 54) gives activation energies of 0.14, 0.35, and 0.42 eV for Cu on Cu (111), Cu(110), and Cu(100), respectively. The Cu(100) estimate agrees reasonably with the experimental values. However, the theoretically calculated Cu(100) value of Hansen *et al.*[52] is roughly half the experimental values.[55]

Segregation of the substrate atoms may occur when the substrate surface free energy is lower than the deposited film surface free energy. It is difficult to estimate the activation energy for this process, since in addition to surface free-energy differences, heats of solution and the elastic size mismatch energy may also play a role.[4] Furthermore, there may be more than one contributing segregation path (see Ref. 56 and references therein). However, we can expect that segregation may be important for Fe and Co on Cu for growth temperatures near and above room temperature because of experimental reports of significant segregation near 400 K for Fe and Co on Cu(100).[16,57–59]

Finally, the upper temperature limit for layer-by-layer equilibrium growth is imposed by requiring an abrupt film/substrate interface. Assuming that interdiffusion occurs through bulk diffusion and with a typical growth time of ~100 s, a growth temperature upper limit is estimated to be near ~0.5 the melting temperature. The upper limit for Cu, Co, and Fe is about 675, 885, and 900 K, respectively. Growth of films at temperatures above this threshold can often produce interdiffused or alloyed layers, even for systems that satisfy Eq. (1).

The limits imposed by these mobilities, combined with the film deposition rate, create a temperature window where equilibrium FM growth may occur.[60,61] For systems, such as Fe/Cu and Co/Cu, which do not satisfy the Eq. (1) criteria for FM growth, layer-by-layer growth may not exist at all. Therefore, in systems of high-surface free-energy metals deposited on low-surface free-energy substrates, we have chosen an alternate approach: deposit the film at low temperature where thermal diffusion is minimal, then anneal the system to a temperature that improves the lattice ordering but does not permit substrate segregation. This technique produces very-high-quality films.[62] Nevertheless, the emphasis of the present study is upon examination of the growth process and characterization of the as-grown film/substrate system. Careful annealing of a film grown at low temperature should be considered an additional, valuable tool to optimize the film quality.

In summary, it is essential to consider the growth kinetics in these metastable thin-film systems. Simple considerations of surface free energies and atomic mobilities provide a foundation for understanding the nonideal growth modes and structures of metastable Fe and Co films on Cu(111), Cu(100), and Cu(110). Furthermore, these ideas are expected to be equally valid and applicable to other thin-film systems.

This paper is organized in six sections. The Introduction (Sec. I) is followed by a review of the experimental methods (Sec. II). Growth on the different substrates is examined individually: Cu(111) (Sec. III), Cu(100) (Sec. IV), and Cu(110) (Sec. V). Within each of these three sections, film growth is discussed (A) in detail for Fe, (B) in detail for Co, and (C) in general for both Fe and Co with an emphasis on common aspects. A brief, general conclusion with specific highlights is given in Sec. VI.

II. EXPERIMENT

The molecular-beam epitaxy (MBE) system used in this work has two ultrahigh vacuum chambers. A long-stroke sample manipulator traverses the central axis of the chambers. The sample can be cooled to 80 K, heated to 1000 K, and rotated by a stepper motor about the main axis of translation. The first chamber contains the sputter ion gun, quadrapole mass spectrometer, LEED system, RHEED system, and metal MBE sources. The system base pressure is 8×10^{-9} Pa. A second adjacent chamber is equipped with a commercial x-ray source and a 150-mm mean-radius hemispherical electron-energy analyzer with input electron optics. The x-ray source and analyzer axis are 90° apart in the plane defined by rota-

DOCKET ALARM Find authenticated court documents without watermarks at docketalarm.com.

tion of the sample normal. The x-ray photoelectron spectroscopy (XPS) and Auger data were obtained with Al $K\alpha$ (1486.6 eV) radiation. The analyzer has a 16-channel parallel detector for improved signal to noise. The geometric acceptance angle of the input electron-optics is $\pm 5°$, which was satisfactory for routine XPS and CO-titration measurements (described below). Improved angular resolution was desirable for forward-scattering measurements and was obtained by inserting an additional aperture, which reduces the acceptance angle to $\pm 2.5°$. The estimated absolute angular accuracy of these measurements is $\pm 1°$ with significantly better relative accuracy of $\pm 0.25°$. Further details of the MBE system are given in previously published work.[62]

All copper substrates were cut from a single-crystal boule using a wire-slurry saw. Each crystal was oriented to better than 0.5° with a diffractometer. The mechanically damaged layer was then removed from both sides of the substrate using an acid polishing instrument.[63] The crystal orientation was then rechecked with the diffractometer. A final, near-mirror finish was obtained by a brief, manual acid polish. The acid polishing solution[64] is formulated to produce optically flat metal surfaces and is based upon a solution of HCl acid, polyethylene glycol, and 2-mercaptobenzimidazole saturated with $CuCl_2$. The removal of much of the damaged layer at the crystal surface is demonstrated by the observation of a weak LEED pattern without any further cleaning or annealing. To remove impurities, the crystal was sputtered using Ar^+ or Ne^+ and annealed to ~ 900 K until no contamination was detectable with XPS and a sharp pattern was obtained with LEED.

All films were grown in a vacuum of 1×10^{-8} Pa or better. Fe was evaporated from a metal oven described elsewhere.[65] Cobalt was deposited from a tungsten-wire-filament evaporator. Typical film growth rates were ~ 2 monolayers/min as measured by an ion-gauge integration system.[62] Film thicknesses were measured by two quartz crystal monitors, symmetrically adjacent to the sample. The calibration of these monitors was done using RHEED oscillations. The average film thickness accuracy is ± 0.10 monolayers (ML) on Cu(100) and Cu(111) and ± 0.15 ML on Cu(110).

Films were routinely checked with XPS to monitor film purity. No attempts were made to correlate film-growth mode with XPS intensity or Auger kinks on account of the dubious nature of this practice for many metal/metal epitaxial systems.[66,67] LEED was used to investigate film structure and morphology.

The crystal structure of the film was investigated using x-ray photoelectron and Auger electron forward-scattering measurements. This technique has recently been used to study many metal-film/metal-substrate systems by several groups.[57,68–71] The primary advantage of this method is its elemental specificity combined with its real-space correspondence to near-neighbor bond direction through enhanced forward-scattering intensity. Strictly speaking, this interpretation of the electron forward scattering is accurate only for electron kinetic energies of several hundred eV or greater. At lower kinetic energies, the electron scattering may be dominated by multiple-scattering effects that distort and obscure simple interpretation. A consistency check is provided by comparing the XPS and Auger angular anisotropies for several different kinetic energies ≥ 0.5 keV: true bond directions will exhibit intensity enhancements independent of the kinetic energy. Therefore, it is generally straightforward to determine the crystal structure of the film from fast and simple XPS or Auger electron angular anisotropy measurements. For pertinent reviews on forward scattering as a diagnostic tool see Refs. 68, 69, and 72.

The crystal structure of the film can also be ascertained by a comparison of XPS and Auger angular anisotropies from deposited films with those observed from pure single crystals. This has the inherent advantage of including multiple-scattering and interference effects. Figure 1 shows polar XPS and Auger angular anisotropies for Cu single crystals with surfaces oriented along the (100), (110), and (111) directions. The XPS and Auger angular anisotropy is defined as the angular-dependent intensity divided by the maximum intensity in the angular scan. The similarity between the anisotropies at the four kinetic energies, Cu $2p_{3/2}$ (552.6 eV), Cu $L_3M_{45}M_{45}$ (916.6 eV), Cu $3s$ (1362.6 eV), and Cu $3p_{3/2}$ (1409.6 eV), for each Cu crystal provides an excellent demonstration of the

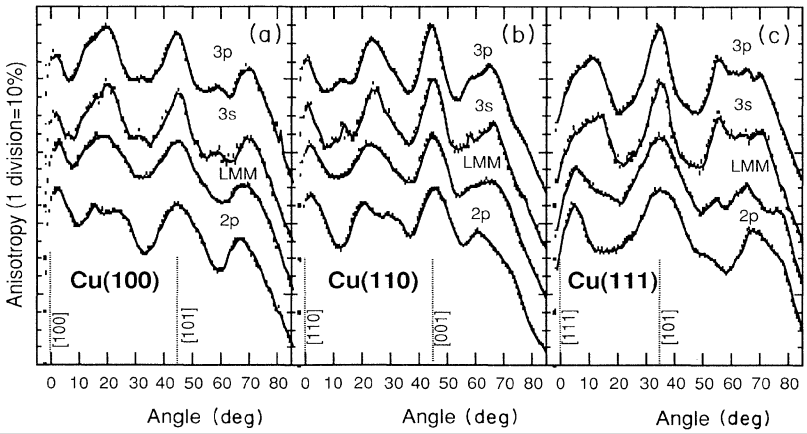

FIG. 1. XPS angular anisotropy vs polar angle for Cu(100), Cu(110), and Cu(111) in the ⟨001⟩, ⟨011⟩, and ⟨1$\bar{2}$1⟩ azimuths, respectively, using Al $K\alpha$ (1486.6 eV) radiation. Spectra are shown for four Cu x-ray and Auger energies: Cu $2p_{3/2}$ (552.6 eV), Cu $L_3M_{45}M_{45}$ (916.6 eV), Cu $3s$ (1362.6 eV), and Cu $3p_{3/2}$ (1409.6 eV). Nearest-neighbor directions are indicated by vertical dotted lines. Anisotropy is defined for each energy as (angular intensity)/(maximum peak intensity). The Cu(100) and Cu(110) 0° peaks appear asymmetric due to the grazing incidence of the Al $K\alpha$ radiation for this orientation.

DOCKET ALARM Find authenticated court documents without watermarks at docketalarm.com.

forward-scattering phenomena. The indicated directions correspond to the crystal normal and to the strong forward-scattering directions that are associated with nearest- and next-nearest-neighbor axes. Scattering from more distant neighbors typically shows weak or no detectable enhancement unless it is compounded by first-order constructive interference effects.[69] A good example of this is the (100) crystal that has consistently strong forward-scattering peaks for all energies along [100] (0°) and [101] (45°) and additional features near 20° and 70°, which disperse slightly with energy. The 20° peak has been shown by simulations[73] to result from both a weak forward-scattering intensity along the [103] (18.4°) direction and a first-order interference maximum coincidentally near 20°, which disperses with electron kinetic energy. The peak near 70° also corresponds to a weak forward-scattering peak combined with a first-order maximum and is symmetric with the 20° maximum about the [101] direction. Similar interference maxima can also be observed in the other crystals, symmetric about the ⟨110⟩ directions.

Forward scattering serves to characterize the film crystallography, but does not provide direct elemental information about the surface layer. To answer difficult questions on film agglomeration and Cu surface segregation, a technique was developed to measure what fraction of the surface was exposed Cu or was "surface Cu." This procedure is referred to as CO titration and has been introduced previously.[62] The procedure is based upon the surface core-level shift of the Cu $2p_{3/2}$ state with adsorption of CO. Since only those Cu atoms exposed at the surface will have core-level shifts, the fraction of the surface that is Cu can be estimated by reference to a clean Cu substrate. To determine the amount of surface Cu for a particular sample, we deposit the film of Fe or Co and then measure the Cu $2p_{3/2}$ peak: (a) without CO, (b) with a saturation dose of CO at ~80 K, and (c) after warming to 300 K to desorb the CO from the Cu. The Cu $2p_{3/2}$ peak contains two contributions: (i) the signal from the surface Cu atoms, which shifts with CO adsorption, and (ii) the signal from nonsurface Cu atoms, which does not shift. To eliminate attenuation by the CO, the peaks are normalized to constant area, then the difference spectra (a)−(b) and (c)−(b) are calculated. (a)−(b) is called the *adsorption cycle* and (c)−(b) the *desorption cycle*. The resulting difference curves show a trough/peak shape that represents of the number of CO-shifted Cu surface atoms. The height of the difference curve for a given film is then compared to identical measurements on a clean Cu substrate with no film. The film/no-film height ratio corresponds to the fraction of the surface that is Cu. The adsorption cycle and desorption cycle estimates should be identical, within the estimated measurement uncertainty (±5%), if the number and kind of surface atoms remains constant after annealing to 300 K with adsorbed CO. Differences in the measurement cycles indicate undetermined instabilities, including film agglomeration and substrate segregation. We report both estimates to demonstrate the systematics of these measurements. However, when the adsorption and desorption measurements differ by more than the measurement uncertainty, we take the average as our best estimate of surface Cu and qualify these systems as metastable.

Generally, CO-titration measurements are made by measuring the Cu $2p_{3/2}$ intensity at a polar angle of 25°. For ideal flat films, measurements should show no change with detection angle in the fraction of the surface that is Cu surface. However, nonideal film growth can produce a variation with detection angle in estimated Cu. This is because measurements performed at 5° off the surface normal integrate contributions from all the Cu surface atoms equally, while measurements made near 80°, for example, will be less sensitive to Cu surface atoms at the bottom of cracks in the film. Therefore, additional angular-dependent CO-titration measurements were occasionally performed at 5°, 45°, 65°, and 80°. The variation in angle of the Cu estimate was then interpreted in terms of the distribution of the Cu surface atoms and the film morphology.

III. GROWTH OF Fe AND Co ON Cu(111)

The growth of Fe and Co on Cu(111) is a particularly rich system that has received considerable attention in the past. The structure of Fe films on Cu(111) has been studied using electron microscopy,[74–78] field-ion microscopy,[70] LEED, and Auger electron spectroscopy (AES).[10,80,81] The magnetic properties have been studied using torque magnetometry,[5–7,82] Mössbauer,[76] and electron-capture spectroscopy.[8] Similar structural studies of Co growth on Cu(111) have used LEED and AES,[18] and nuclear magnetic resonance (NMR),[83–87] surface-extended x-ray-absorption fine structure (SEXAFS),[88,89] x-ray scattering,[90] and XPS forward scattering.[91] The magnetic properties of Co/Cu(111) have been measured by torsion magnetometry,[92] ultraviolet photoelectron spectroscopy,[18,93] surface magneto-optic Kerr effect,[94,95] and torsion oscillation magnetometry.[96]

Table I shows that there is a very close lattice match to the Cu(111) surface net for both fcc and bcc phases of Fe, and both fcc and hcp phases of Co. In addition to the lattice match, the crystalline phase of the film is controlled by the epitaxial strain in the film. The equilibrium

TABLE I. Epitaxy of Fe and Co on Cu(111).

Material/ symmetry	Lattice constant (Å)	Nearest neighbor (Å)	Surface cell mismatch (%)	Interlayer spacing (Å)
fcc Cu(111)	3.61	2.55		2.08
fcc Fe(111)	3.59	2.54	−0.8	2.07
bcc Fe(110)	2.87	2.48	+3.4	2.03
fcc Co(111)	3.54	2.50	−3.9	2.05
hcp Co(0001)		2.51	−3.2	2.03

DOCKET ALARM Find authenticated court documents without watermarks at docketalarm.com.

configuration of the strained film is predicted by minimizing the system free energy for all possible film crystalline phases, orientations, strains, and dislocations,[97,98] However, even this model of lattice mismatch and film elasticity is oversimplified, because it only considers continuous films. We will show below that there is no single epitaxial phase for Fe and Co on Cu(111). The epitaxial phase of the film depends on the growth temperature and the film thickness.

A. Fe/Cu(111)

Fe films were prepared at substrate growth temperatures of 80 and 300 K. The structure of these films was examined for thicknesses up to 8 ML. The fraction of Cu in the exposed surface was measured with both the adsorption and desorption CO-titration sequence as described above. These values were typically found to agree within 5%, which we believe is near our experimental accuracy. Therefore, we only report the average values. Figure 2 shows the fraction of Cu in the exposed surface versus film thickness. The fraction of Cu in the exposed surface increases with growth temperature and decreases with deposited Fe thickness. The data show that after deposition of about 3 ML of Fe grown at 80 K and 5 ML of Fe grown at 300 K the surface is 5% and 12% Cu, respectively. This agrees well with scanning tunneling microscopy (STM) estimates of 10% of the Cu substrate exposed for 4 ML of Fe deposited at 300 K.[99] Furthermore, annealing these films shows that they are stable. This thermal stability is demonstrated by the observations that a 2.3-ML grown at 80 K and a 5.6-ML film grown at 300 K show no increase in the fraction of Cu in the exposed surface for anneals of 300 K over the growth temperature. The large fraction of Cu at the surface indicates the Fe film growth is not an ideal layer-by-layer manner. This growth mode is in contrast to most of the literature,[5–10] which reports room-temperature FM growth of Fe/Cu(111).

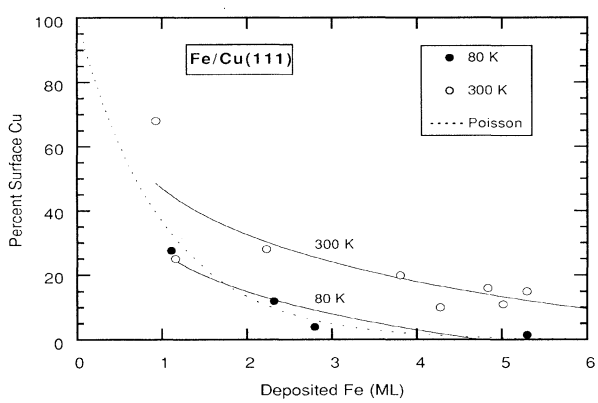

FIG. 2. The fraction of Cu in the surface for Fe deposited on Cu(111) at 80 and 300 K. Coverage is determined by the CO-titration technique using the average of adsorption and desorption measurements for 25° detection angle. Solid curves show an exponential fit to the drop in the measured fraction of Cu in the surface. The dotted line indicates the fraction of Cu in the surface for random substrate coverage according to Poisson statistics (see text for interpretation).

For comparison to the measured values, Fig. 2 shows the predicted values of the fraction of Cu in the exposed surface for the Poisson model. The Poisson model assumes random deposition on a simple cubic lattice. The direct comparison of the measured values with the Poisson model should be done with caution because the simple cubic lattice does not explicitly include the fcc(111) threefold adsorption geometry or stacking faults. If the adatoms have zero mobility, this model implies unphysical vacancies and overhangs. Relaxing this constraint and allowing the second layer adatoms to drop down into one of three possibly unfilled nearest-neighbor sites increases the substrate coverage to 52%, 21%, and 4% for depositions of 0.5, 1.0, and 2.0 ML, respectively. Comparing these new estimates with the simple cubic model prediction (Fig. 2) decreases the agreement, particularly for depositions above 1.5 ML. Alternatively, if the adatoms are somewhat mobile but cannot diffuse over a step and (or) the coverage is not random but locally correlated as occurs with small cluster nucleation, the simple cubic lattice Poisson estimate may be more appropriate. Examples of these types of growth are Pt/Pt(111) at 400 K (Refs. 100 and 101) and Fe, Co, and Cu on Cu(100) at 80 K.[102] Keeping these possibilities in mind, we have chosen always to plot the Poisson model estimates with the CO-titration measurements. The Poisson model estimate serves as a guideline for comparison between different materials, symmetries, and growth temperatures.

The crystalline structure of the Fe film was determined using forward scattering. Figure 3 plots the XPS angular anisotropies of Fe $3p_{3/2}$ (1431.6 eV) for films grown at 80 and 300 K and for depositions from about 1–7 ML.

The films deposited at low temperature, 80 K, show the evolution of a bcc Fe phase, which is indicated by a peak in the XPS angular anisotropy at 45°. The weak, broad rise near 45° with no 0° feature show the 1.0-ML film is nearly flat. The rise of a peak at 0° for a 2.3-ML film signifies the start of the third bcc layer, which is consistent with nearly layer-by-layer growth. Increasing the film thickness shows increasing structure in the angular anisotropies that indicate a bcc film.

A 1.0-ML film deposited at 80 K has a LEED pattern that is $p(1\times1)$ and is threefold symmetric. The LEED spots alternate between fuzzy and sharp as a function of the beam energy. A 2.3-ML Fe film has a similar LEED pattern with a brighter background and very broad spots. These LEED patterns indicate that the atoms sit largely in lattice sites but many steps are present. Films that are annealed to 350 K have sharpened LEED spots and a clearer three-fold symmetry. In contrast, the XPS angular anisotropy shows little change in structure for films that are annealed, indicating that short-range order in the films changed little. A film thicker than 4 ML has a LEED pattern that is sixfold symmetric with broad spots. In addition, the LEED pattern has new diffuse spots (these spots are similar to those labeled *B* in Fig. 4, which are observed in room temperature grown films). Annealing the films sharpens the LEED pattern but less so for thicker Fe films. A 5.6-ML film grown at 80 K and

DOCKET ALARM Find authenticated court documents without watermarks at docketalarm.com.

DOCKET ALARM

Explore Litigation Insights

Docket Alarm provides insights to develop a more informed litigation strategy and the peace of mind of knowing you're on top of things.

Real-Time Litigation Alerts

Keep your litigation team up-to-date with **real-time alerts** and advanced team management tools built for the enterprise, all while greatly reducing PACER spend.

Our comprehensive service means we can handle Federal, State, and Administrative courts across the country.

Advanced Docket Research

With over 230 million records, Docket Alarm's cloud-native docket research platform finds what other services can't. Coverage includes Federal, State, plus PTAB, TTAB, ITC and NLRB decisions, all in one place.

Identify arguments that have been successful in the past with full text, pinpoint searching. Link to case law cited within any court document via Fastcase.

Analytics At Your Fingertips

Learn what happened the last time a particular judge, opposing counsel or company faced cases similar to yours.

Advanced out-of-the-box PTAB and TTAB analytics are always at your fingertips.

API

Docket Alarm offers a powerful API (application programming interface) to developers that want to integrate case filings into their apps.

LAW FIRMS

Build custom dashboards for your attorneys and clients with live data direct from the court.

Automate many repetitive legal tasks like conflict checks, document management, and marketing.

FINANCIAL INSTITUTIONS

Litigation and bankruptcy checks for companies and debtors.

E-DISCOVERY AND LEGAL VENDORS

Sync your system to PACER to automate legal marketing.